Supplement of Biogeosciences, 18, 2957–2979, 2021
https://doi.org/10.5194/bg-18-2957-2021-supplement

Biogeosciences
Open Access

Supplement of

Climate change and elevated CO_2 favor forest over savanna under different future scenarios in South Asia

Dushyant Kumar et al.

Correspondence to: Dushyant Kumar (dushyant.kumar@senckenberg.de)

aDGVM2 model description

The aDGVM2 is an individual-based dynamic vegetation model that simulates growth, reproduction and mortality of individual plants at representative 1 ha stands. The model is process-based and represents physiological, phenological and demographic processes. It integrates from the leaf level to the plant level and from there to the community or stand level. Simulation results can be used to aggregate communities on yet larger spatial scales, for example to derive biomes. To simulate leaf-level ecophysiological processes the Collatz et al. (1991, 1992) implementation of the Farquhar photosynthesis scheme (Farquhar et al., 1980), combined with the Ball et al. (1987) implementation of stomatal conductance. While in previous model versions, leaf-level ecophysiological rates were calculated at stand-level ignoring individual-specific physiological differences, the updated model version used in this study, calculates leaf-level ecophysiological rates at a daily time resolution for each individual plants (also see Section 2.2). The calculation of the CO_2 compensation point (gammastar) depicts the dependency of carboxylation vs. oxygenation as a function of oxygen partial pressure and temperature (the latter via a Q10-function), and the CO_2 compensation point is then used further to determine J_e (electron transport-limited photosynthesis, this also takes into account photosynthetically active radiation, i.e., PAR) and J_c (CO_2 concentration limited photosynthesis, this also accounts for temperature-dependent V_{cmax}). In the aDGVM2 version developed for this study, V_{cmax}, the maximum carboxylation velocity is temperature-dependent (Equation 4) and reaches a peak around 37°C for C_3 plants and 42°C for C_4 plants. Beyond the temperature optimum, V_{cmax} declines at higher temperatures. This mimics the combined effect of decreasing enzyme activity due to the increased competitory binding of O_2 at higher temperatures and eventually enzyme degradation at very high temperatures. Effects caused by changing atmospheric CO_2 concentrations and rising temperatures, including changes in carboxylation vs. oxygenation, are therefore explicitly captured by the implemented photosynthesis scheme. In addition, effects of water limitation on stomatal conductance are represented by the Ball et al. (1987) implementation of stomatal conductance that ties photosynthesis to stomatal conductance via a diffusion-gradient definition.

The design of aDGVM2 allows tracking of state variables such as biomass, height, leaf area and photosynthetic rates of individual plants. In aDGVM2, each plant is characterized by a specific and potentially unique combination of trait values that influence how a plant performs under given biotic and abiotic conditions. It allows plant communities to adapt to their environment by dynamically changing their trait composition constrained by trade-offs between traits. These traits describe plant type (grassy or woody), leaf characteristics (specific leaf area, leaf longevity), leaf phenology (evergreen or deciduous), hydraulic characteristics (risk of xylem cavitation), plant architecture (carbon allocation strategy, root and crown shape, wood density), response to fire, reproduction and mortality (Langan et al., 2017; Scheiter et al., 2013). The aDGVM2 implements plant physiology models typically used in DGVMs (Prentice et al., 2007). Fire systematically removes aboveground grass biomass while aboveground tree biomass removal is related to tree height (Higgins et al., 2008; Scheiter and Higgins, 2009). Plants with trait combinations that allow sufficient growth and reproduction rates can produce seeds and contribute their trait values to the community trait pool. Seeds can randomly mutate or exchange trait values, thereby allowing recombination within the community trait pool. Seeds are randomly drawn from the community trait pool and added to the plant population as seedlings. Plants with insufficient performance fail to contribute seeds to the seed bank and disappear from the population. Plant growth is constrained by light and water competition. Light competition is simulated by considering the impacts of neighboring plants on the light available to a target plant. Water competition is simulated via water uptake of plants from a common layered soil water pool. The probability of an individual's mortality increases if its annual carbon balance is negative. The aDGVM2 also includes a representation of shrubs as multi-stemmed woody plants, based on the stem number of individual woody plants as dynamic trait which emerge as adaption to dry conditions (Gaillard et al., 2018). This trait allows simulation of shrubs vs. trees based on a functional trade-off between augmented access to soil water resources vs. height growth. It simulates shrubs as multi-stemmed woody plants. We define all woody individuals with a stem number between one and three as trees, whereas individuals with more than three stems are categorized as shrubs. The classification of individuals into these two categories is done a posteriori, based on the model results. Stem numbers in a woody plant are emerging based on water availability, light availability and fire activity. Rapid height growth is characteristics of single-stemmed trees whereas augmented efficiency of water uptake due to higher sapwood area per unit of woody biomass is characteristic for multi-stemmed shrubs.

Table S1. List and description of traits that are optimized by the genetic optimization algorithm during model simulation. Values for trees and C_4 grasses were taken from Langan et al. (2017). C_3 grasses were included for this study and values of C_4 grasses were taken for model parametrization. 'na' indicates that this trait is not used for grasses."(-)" indicates unitless.

Description of traits	Woody		C_4-grass		C_3-grass	
	min	max	min	max	min	max
Matric potential at 50% loss of conductance, P50 (MPa)	-3	-0.2	-3	-0.2	-3	-0.2
Allocation to roots (Fraction)	0.2	0.4	0.2	0.8	0.2	0.8
Allocation to leaves (Fraction)	0.35	0.5	0.2	0.8	0.2	0.8
Allocation to stem (Fraction)	0.25	0.35	0	0	0	0
Allocation to bark (Fraction)	0.001	0.05	0	0	0	0
Allocation to storage (Fraction)	0.1	0.4	0.1	0.4	0.1	0.4
Allocation to reproduction (Fraction)	0.05	0.2	0.05	0.2	0.05	0.2
Phenology (rain/summer green, evergreen) (-)	0	1	0	1	0	1
Phenology (deciduous or evergreen) (-)	0	1	1	1	1	1
Rain threshold for plant activity (-)	-3	-0.2	-3	-0.2	-3	-0.2
Rain threshold for plant dormancy (-)	-3	-0.2	-3	-0.2	-3	-0.2
Light threshold for plant activity (-)	0.1	2	0.1	2	0.1	2
Light threshold for plant dormancy (-)	6	14	6	14	6	14
Parameter for height calculation (-)	0.4	0.4	na	na	na	na
Parameter for height calculation (-)	0.4	0.5	na	na	na	na
Parameter for root form (-)	0.01	10	0.01	10	0.01	10
Parameter for root form (-)	-1	20	1	20	1	20
Maximum rooting depth (m)	0.3	3.6	0.3	2.4	0.3	2.4
Seed weight (kg)	0.001	0.05	0.001	0.05	0.001	0.05
Parameter for canopy form (Fraction)	21	25	20	60	20	60
Storage to stem allocation after fire (Fraction)	0.2	0.4	0	0	0	0
Storage to leaf allocation after fire (Fraction)	0.6	0.9	0.6	0.9	0.6	0.9
Stem Count (Number)	1	10	1	1	1	1

Table S2. List and description of traits that are constant during the model simulation and are not optimized by the genetic optimization algorithm. Values for trees and C_4 grasses were taken from Langan at al. (2017). C_3 grasses were included for this study and values of C_4 grasses were taken for model parametrization. ‘na’ indicates that this trait is not used for grasses and ’*’ denotes new parameters. "-" indicates unitless.

Description of traits	Woody	C_4 Grass	C_3 Grass
Mortality due to negative carbon balance (Fraction)	0.3	0.2	0.2
Mortality due to low height (m)	0.1	0.05	0.05
Mortality due to mechanic instability 1 (Fraction)	10	5	5
Mortality due to mechanic instability 2 (Fraction)	6	6	6
Topkill constants parameter 1 (-)	1.48	0	0
Topkill constants parameter 2 (-)	3.30698	0	0
Topkill constants parameter 3 (-)	0.02618	0	0
Ball berry equation parameter 1 (-)	9	5.48	9
Ball berry equation parameter 2(μmol/m^{2}s)	0.01	0.02	0.01
Maintenance respiration parameter (Fraction)	0.015	0.025	0.015
Growth respiration parameter (Fraction)	0.35	0.35	0.35
Fraction of leaf biomass that respires (Fraction)	1	0.01	0.01
Fraction of wood biomass that respires (Fraction)	0.1	0.01	0.01
Fraction of root biomass that respires (Fraction)	0.01	0.01	0.01
Parameter for respiration model (kgC kgN^{-1}Day^{-1})	0.218	0.218	0.218
C:N ratio of woody biomass (Fraction)	150	120	120
C:N ratio of woody biomass (Fraction)	60	120	120
Lower temperature limits for efficient carboxylation ($^\circ$C)	-10*	15*	-10*
Upper temperature limits for efficient carboxylation ($^\circ$C)	36*	45*	36*

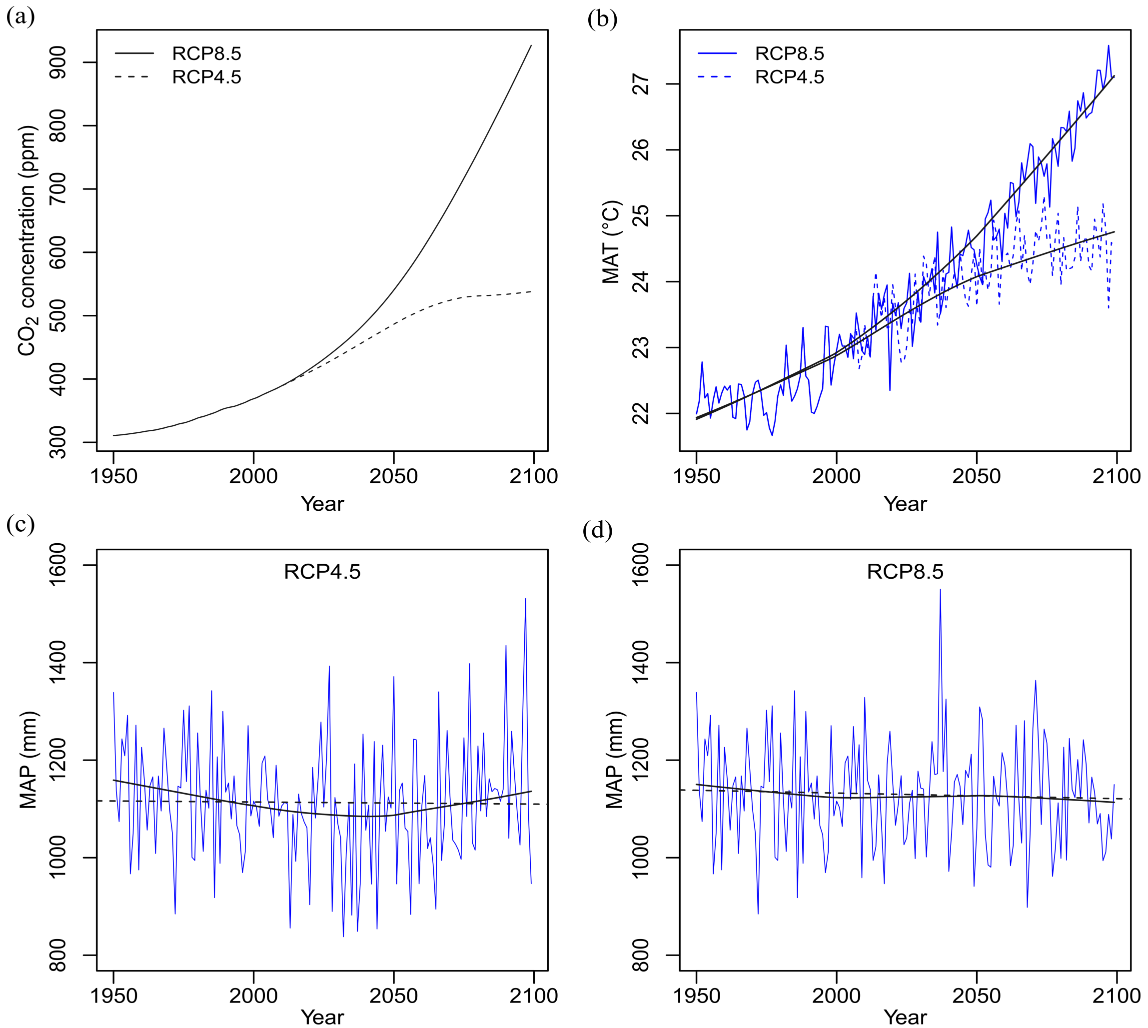

Figure S1. Time series represent (a) CO2 concentration under RCP4.5 and RCP8.5; (b) mean annual temperature under RCP4.5 and RCP8.5; (c) mean annual precipitation for RCP4.5 and (d) mean annual precipitation for RCP8.5 for South Asia between 1951 and 2099. In (b), (c) and (d) the black solid line represents a smoothed non-linear fit (LOWESS), and in (c) and (d) the black dashed line represents a linear smoothed fit (LOWESS) to the data. Mean annual precipitation and mean annual temperature were derived from GFLDM2M simulations.

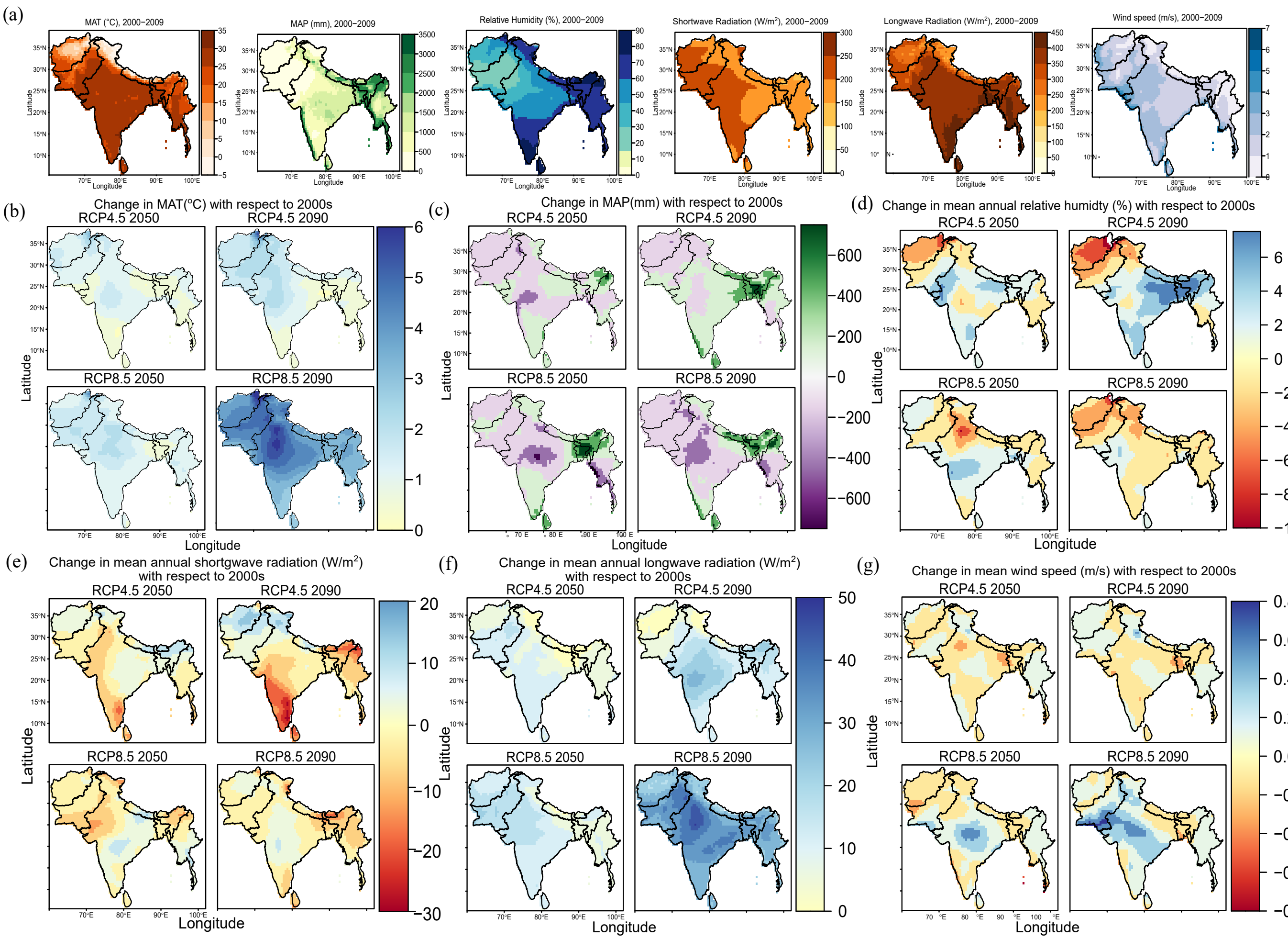

Figure S2. (a) Baseline mean of the climate variables (2000-2009),projected change in (b) mean annual temperature (MAT), and (c) mean annual precipitation (MAP), (d) mean annual relative humidity, (e) mean annual short-wave radiation, (f) mean annual long-wave radiation and (g) mean annual wind speed until the 2050s and the 2090s, relative to the baseline (2000s-2009).

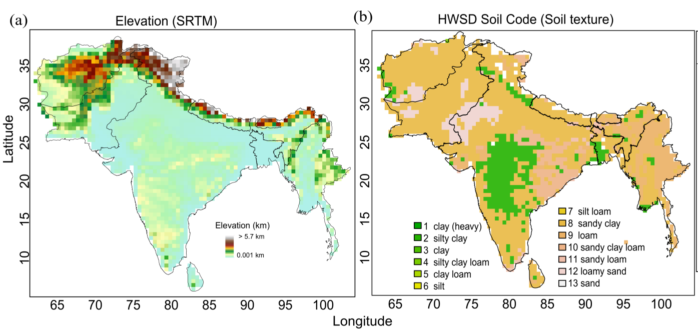

Soil properties

Soil Code HWSD	θ_{swc} ($m^3\ m^{-3}$)	K_{sat} ($m\ hr^{-1}$)	φ_{soil} (m)	r	rc ($m^3\ m^{-3}$)
1	0.50	0.00133	0.405	12.13	0.020
2	0.52	0.0037	0.49	10.21	0.035
3	0.52	0.0037	0.49	10.21	0.041
4	0.51	0.0057	0.356	8.16	0.027
5	0.48	0.0043	0.63	8.16	0.015
6	0.48	0.022	0.63	3.63	0.068
7	0.48	0.0161	0.786	5.42	0.075
8	0.44	0.0014	0.153	9.39	0.040
9	0.46	0.0155	0.478	6.10	0.109
10	0.43	0.0113	0.356	6.77	0.056
11	0.45	0.0503	0.218	4.73	0.090
12	0.46	0.0967	0.09	4.32	0.090
13	0.46	0.1081	0.121	3.91	0.121
Nachtergaele et al..(2012)	Saxton & Rawls (2006)	Saxton & Rawls (2006)	Clapp & Hornberger (1978)	Boone et al. (2004)	Rawls et al. (1982)

θ_{swc} : saturated water content; rc: residual soil water content.
K_{sat} : saturated hydraulic conductivity; φ_{soil} : Saturation suction;
r: shape parameter describing how percolation decreases as soil dries

Figure S3. (a) Shuttle Radar Topography Mission (SRTM) elevation data (Jarvis et al., 2008) and (b) spatial distribution of soil texture according to the Harmonized World Soil Database (HWSD soil code) (Nachtergaele et al., 2009) and corresponding soil properties in the table, used in current study.

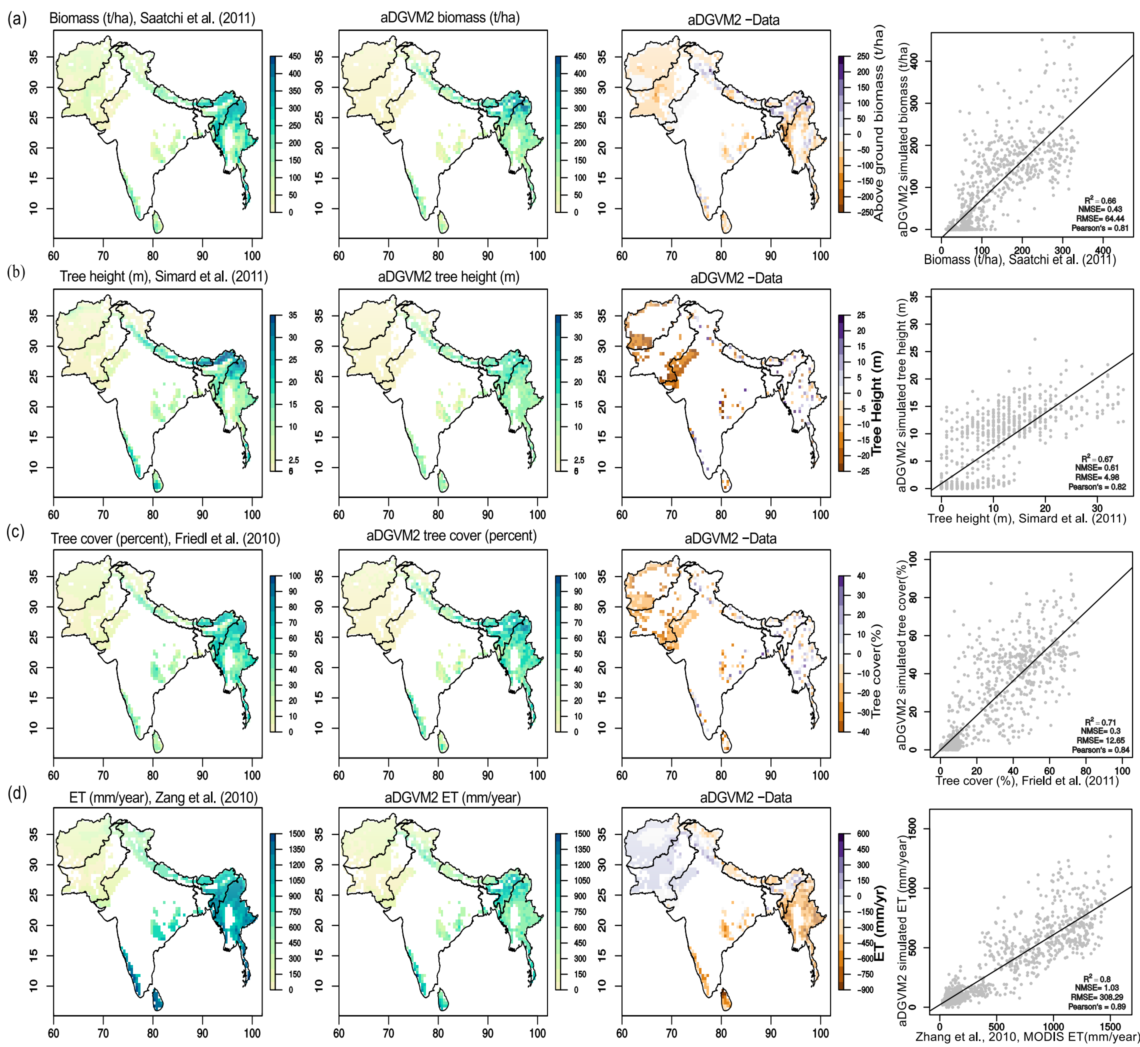

Figure S4. Comparison between aDGVM2 results and remote sensing products when removing areas with more than 50% land use cover for (a) simulated biomass and Saatchi et al. (2011) biomass, (b) simulated tree height and Simard et al. (2011), (c) simulated tree cover and Friedl et al. (2011) tree cover and (d) simulated evapotranspiration and Zang et al. (2010) evapotranspiration. In the figure the first column shows the remote sensing products, the second column shows aDGVM2 results and the third column shows the difference between simulation and data and the fourth column shows the scatter plot between simulated state variable and benchmarking data. NMSE and RMSE are normalized mean square error and root mean square error, respectively. In fourth column, each points represents one grid cell in the study region.

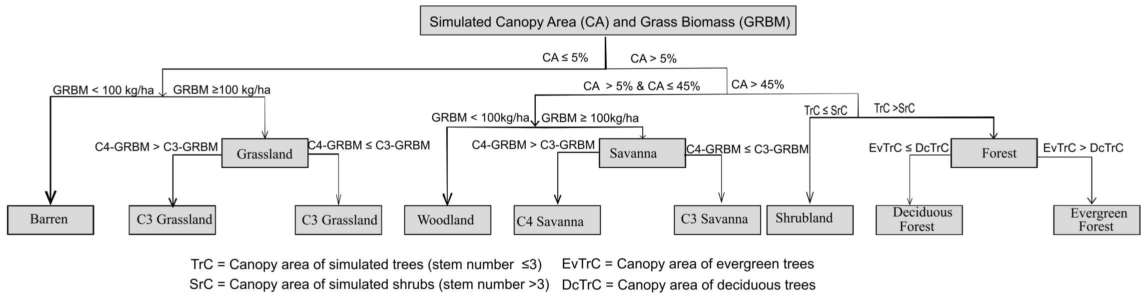

Figure S5. Flow chart illustrating classification of simulated vegetation into biomes using canopy area (CA) of different woody vegetation types and grass biomass(GRBM). Simulated stem numbers were used to distinguish between shrubs and trees.

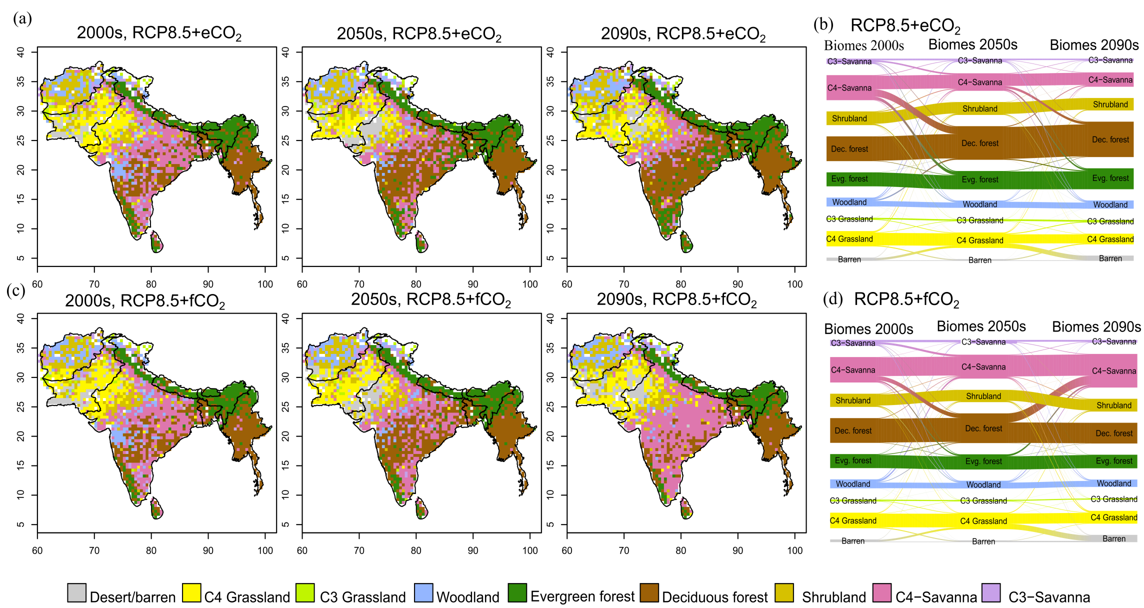

Figure S6. Simulated biome distribution for the 2000s, 2050s and 2090s under (a) RCP8.5+eCO_2 and (c) RCP8.5+fCO2, and Sankey diagrams showing the transition between biomes from the 2000s to the 2050s and the 2050s to the 2090s under (b) RCP8.5+eCO_2 and (d) RCP8.5+fCO2. See Figure 3 for simulated biome distribution under RCP4.5.

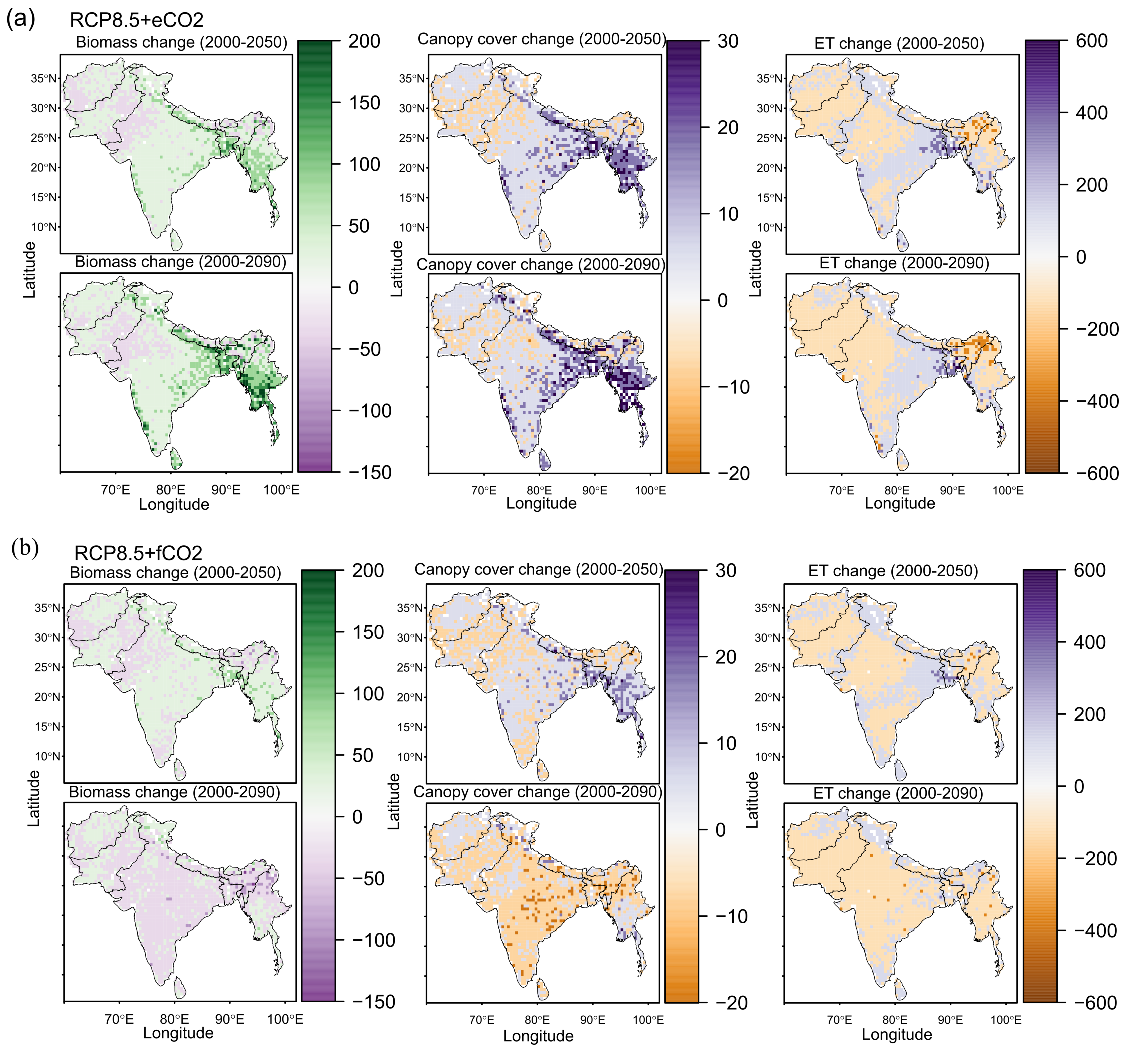

Figure S7. Projected change in biomass, canopy area and evapotranspiration (ET) between the 2000s and 2050s, and between the 2000s and 2090s under (a) RCP84.5+eCO_2 and (b) RCP8.5+fCO_2.

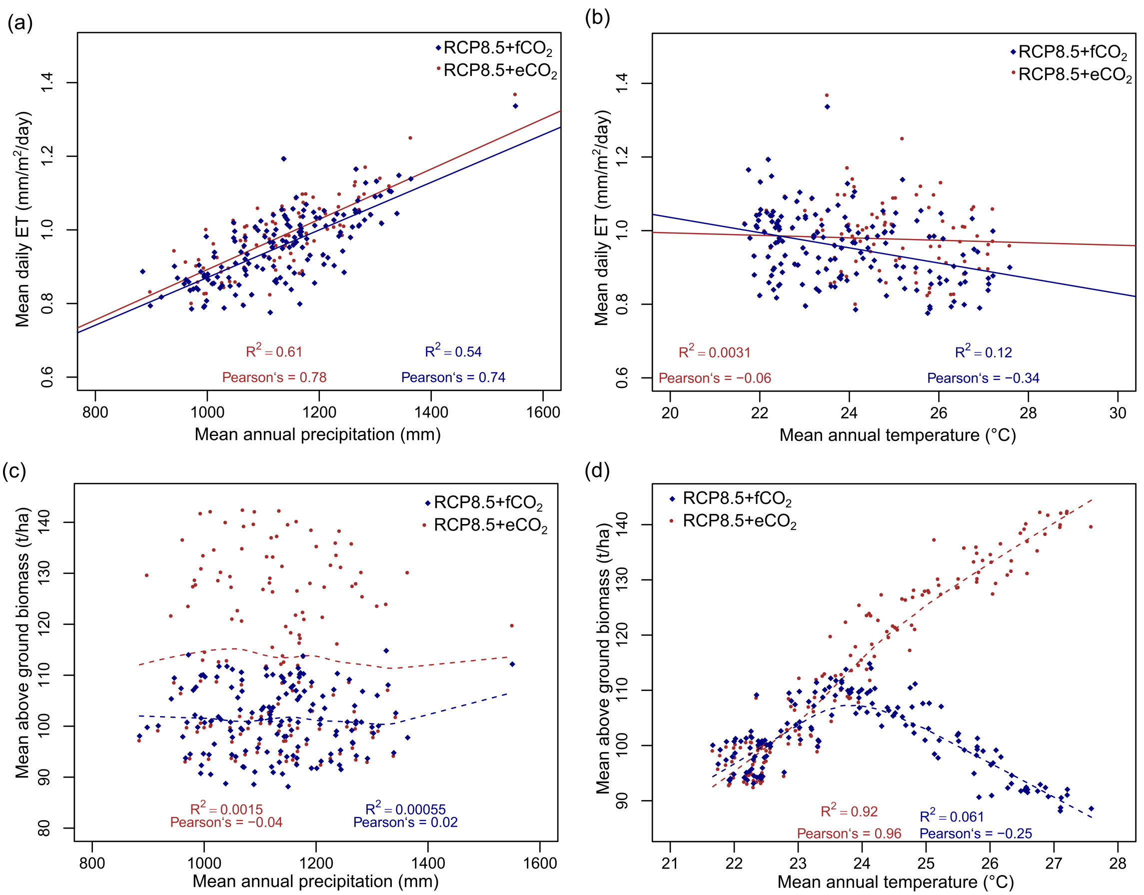

Figure S8. Relationship between (a) evapotranspiration (ET) and mean annual precipitation (MAP), (b) ET and mean annual temperature (MAT), (c) mean above ground biomass and MAP and (d) mean above ground biomass and MAT under RCP8.5.. The lines (both solid and dotted) in all figures represent the best-fit regression line. The dots represent spatially averaged ET (a, b) and biomass (c, d) for each year from 1950 to 2099. See Figure 6 for results under RCP4.5.

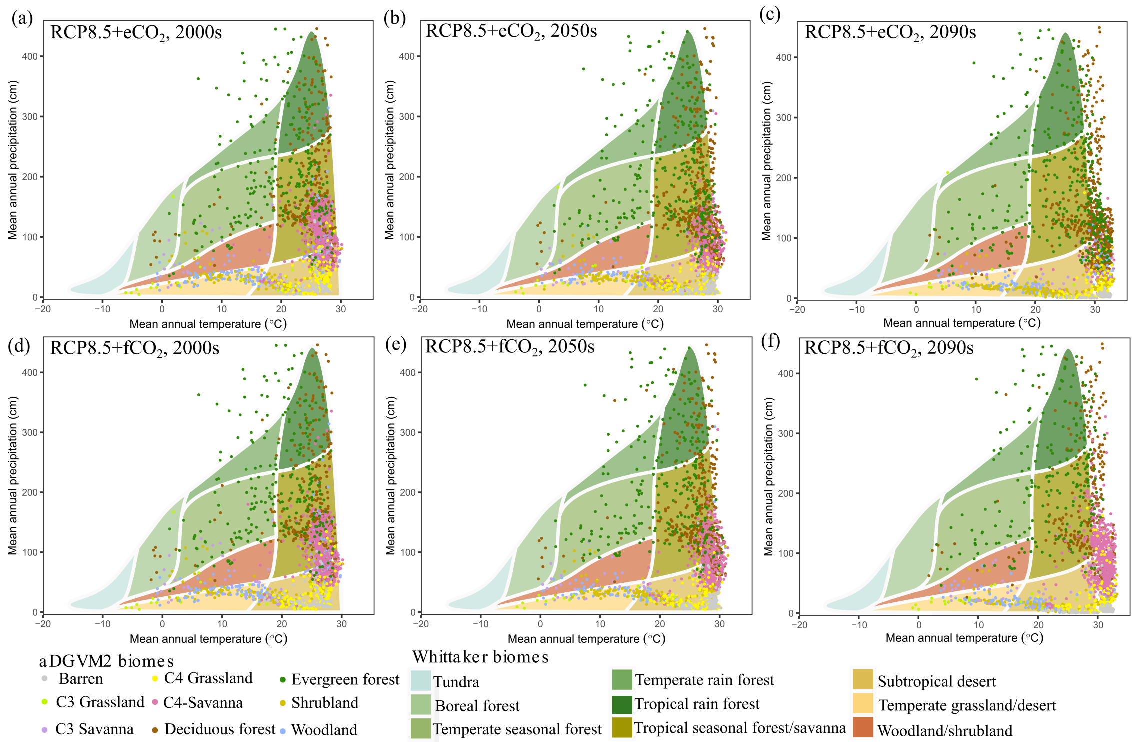

Figure S9. Simulated climatic niches of biomes for the period of (a) 2000s, (b) 2050s and (c) 2090s under RCP8.5+ eCO_2 and (d) 2000s, (e) 2050s and (f) 2090s under RCP8.5+fCO_2. The simulated biomes are overlaid on the climate envelopes of Whittaker's biomes and are plotted following Ricklefs (2008) and Whittaker (1975).

References

Ball, J. T., Woodrow, I. E., and Berry, J. A.: A model predicting stomatal conductance and its contribution to the control of photosynthesis under different environmental conditions, in: Progress in photosynthesis research, pp. 221–224, Springer, https://doi.org/10.1007/978-94-017-0519-6_48, 1987.

Collatz, G. J., Ball, J. T., Grivet, C., and Berry, J. A.: Physiological and environmental regulation of stomatal conductance, photosynthesis and transpiration: a model that includes a laminar boundary layer, Agricultural and Forest meteorology, 54, 107–136, https://doi.org/10.1016/0168-1923(91)90002-8, 1991.

Collatz, G. J., Ribas-Carbo, M., and Berry, J. A.: Coupled photosynthesis-stomatal conductance model for leaves of C4 plants, Functional Plant Biology, 19, 519–538, https://doi.org/10.1071/pp9920519, 1992.

Farquhar, G. D., von Caemmerer, S. v., and Berry, J. A.: A biochemical model of photosynthetic CO_2 assimilation in leaves of C_3 species, Planta, 149, 78–90, https://doi.org/10.1007/bf00386231, 1980.

Gaillard, C., Langan, L., Pfeiffer, M., Kumar, D., Martens, C., Higgins, S. I., and Scheiter, S.: African shrub distribution emerges via height—Sapwood conductivity trade-off., https://doi.org/10.1111/jbi.13447, 2018.

Higgins, S. I., Bond, W. J., Trollope, W. S., and Williams, R. J.: Physically motivated empirical models for the spread and intensity of grass fires, International Journal of Wildland Fire, 17, 595–601, https://doi.org/10.1071/wf06037, 2008.

Jarvis, A., Reuter, H. I., Nelson, A., and Guevara, E.: Hole-filled SRTM for the globe Version 4, available from the CGIAR-CSI SRTM 90m Database, 2008.

Langan, L., Higgins, S. I., and Scheiter, S.: Climate-biomes, pedo-biomes or pyro-biomes: which world view explains the tropical forest–savanna boundary in South America?, Journal of Biogeography, 44, 2319–2330, https://doi.org/10.1111/jbi.13018, 2017.

Nachtergaele, F., van Velthuizen, H., Verelst, L., Batjes, N., Dijkshoorn, K., Van Engelen, V., Fischer, G., Jones, A., Montanarella, L., and Petri, M.: Harmonized world soil database (version 1.1), FAO, Rome, Italy & IIASA, Laxenburg, Austria, 2009.

Scheiter, S. and Higgins, S. I.: Impacts of climate change on the vegetation of Africa: an adaptive dynamic vegetation modelling approach, Global Change Biology, 15, 2224–2246, https://doi.org/10.1111/j.1365-2486.2008.01838.x, 2009.

Scheiter, S., Langan, L., and Higgins, S. I.: Next-generation dynamic global vegetation models: learning from community ecology, New Phytologist, 198, 957–969, https://doi.org/10.1111/nph.12210, 2013.